

Rapid and efficient chiral separation of nateglinide and its L-enantiomer on monolithic molecularly imprinted polymers

Junfa Yin^a, Gengliang Yang^{a,b,*}, Yi Chen^a

^a Center for Molecular Science, Institute of Chemistry, Chinese Academy of Sciences, Beijing 100080, PR China

^b College of Pharmacy, Hebei University, Baoding 071002, PR China

Received 20 January 2005; received in revised form 14 June 2005; accepted 27 June 2005

Available online 19 July 2005

Abstract

A monolithic molecularly imprinted polymer (monolithic MIP) was designed and prepared for chiral separation of nateglinide and its L-enantiomer. The enantiomers were rapidly separated on this novel monolithic MIP based chiral stationary phase (MIP-CSP), whereas the enantioseparation was not obtained on the non-imprinted polymer (NIP). Chiral recognition was found to be dependent on the stereo structures and the arrangement of functional groups of the imprinted molecule and the cavities on MIP. Thermodynamic data ($\Delta\Delta H$ and $\Delta\Delta S$) obtained by Van't Hoff plots revealed an enthalpy-controlled enantioseparation. The binding capacity was evaluated by frontal analysis. Monolithic nateglinide-MIP had an effective number of binding sites $B_t = 41.15 \mu\text{mol g}^{-1}$ with a dissociation constant of $K_d = 7.40 \text{ mM}$. The morphological characteristics of the monolithic MIP were investigated by pore analysis and scanning electron microscope (SEM). Results showed that both mesopores and macropores were formed in the monolith. Over all, this study presents a new and practical possibility for providing high rates of mass transfer, fast separations and high efficiencies without the pressure constraints of the traditional bulk molecularly imprinted polymers, through the monolithic MIPs.

© 2005 Elsevier B.V. All rights reserved.

Keywords: Molecularly imprinted polymer; Monolithic column; Chiral separation; Chiral stationary phases; Nateglinide

1. Introduction

The molecular imprinting technique, first proposed by Wulff et al. in 1972 [1], has recently been developed and shown appropriate for preparation of tailor-made chiral stationary phases (CSPs) [2–7]. Molecularly imprinted polymer (MIP) based CSPs are synthesized by the polymerization of cross-linker and the assembling complex of the templates (optically active molecules) and the functional monomers. Once the polymer is obtained, the imprinted molecules are removed leaving cavities complementary in size, shape and matrix of functional groups to the analyte, allowing it to selectively rebind the template molecules. As a consequence, the final MIP-CSPs are able to discriminate the optically active template from its enantiomer.

The traditional bulk MIP has to be grounded and sieved to the desired particles with appropriate size. This tedious and time-consuming process often produces particles that are irregular in size and shape, resulting in minimal chiral separation with low column effect. In addition, some interaction sites are destroyed during grinding, and thus lead to lower MIP loading capacity with respect to theoretical values. Due to these limitations, the traditional bulk MIPs are not absolutely accepted and used in analytical laboratories. In order to overcome these problems, various strategies have been proposed for direct preparation of MIPs. Uniformed spherical particles have been obtained by using multi-step swelling method [8], suspension polymerization [9], imprinting on surfaces of spherical polymer or silica [10,11], etc.

Monolithic MIPs are expected to improve the separation and enable direct analysis with high-speed and high-performance. In recent years, the uses of monolithic media for superior chromatographic separation in high-performance

* Corresponding author. Tel.: +86 10 82627290.

E-mail address: glyang@iccas.ac.cn (G. Yang).

liquid chromatography (HPLC) and capillary electrochromatography (CEC) have attracted considerable attention [12–14]. Moreover, both monolithic silica columns and monolithic polymer columns are currently commercially available. Their greater porosity, and hence good permeability, and high surface area are well suited for both small molecules and large biopolymers. MIP monoliths have been designed and prepared by in situ polymerization in the 1990s. Matsui et al. [15,16] synthesized continuous rods of molecularly imprinted polymers for chromatographic separations using an in situ method to make the preparation procedure simple and easy to perform. Subsequently, monolithic MIP stationary phases used for CEC have intensively studied [17,18]. Huang et al. [19,20] have developed an improved method for the preparation of short and disk monolithic MIP columns with both satisfactory flow-through properties and high resolution for separation of enantiomers and diastereomers. More recently, Kim and Guiochon [21] compared the thermodynamic properties of monolithic and bulk MIPs against Fmoc-L-tryptophan. Examination of the thermodynamic properties on these two different MIPs showed there were at least three types of binding sites (i.e. the high, the intermediate and the low energy sites) that coexist on the surface. The results suggested that from a thermodynamic point of view, monolithic MIPs could provide a better enantioseparation through the reduction of the density of nonselective interactions of the template with the polymer matrix.

This study describes the use of monolithic MIP-CSPs for chiral separation of nateglinide and its L-enantiomer. Nateglinide [*N*-(*trans*-4-isopropyl-cyclohexylcarbonyl)-D-phenylalanine] (Fig. 1) is a novel non-sulfonylurea oral antidiabetic drug for the treatment of type II diabetes mellitus. Nateglinide can reportedly stimulate a rapid, transient secretion of insulin from the pancreatic β -cells which is dependent on ambient glucose concentrations [22]. An oral dose of 1.6 mg kg^{-1} nateglinide can induce

a 20% decrease in blood glucose, whereas approximately 100 mg kg^{-1} of L-enantiomer is required for equal potency. Therefore, developing a more efficient chiral separation procedure for nateglinide and its enantiomer is worthwhile [23]. Our previous work investigates the separations of nateglinide and L-enantiomer using conventional chiral column (SUMICHIRAL-OA-3300) and bulk nateglinide-MIP column [24,25]. The peaks in chromatograms were commonly asymmetric and broad owing to both non-linear adsorption or desorption and slow mass transfer process. The irregular size and shape, the low surface area together with low mesoporosity, lead to low template recognition in the subsequent binding experiments owing to slow analyte diffusion to sites located in micropores. The present study develops a promising and simple method for the preparation of the monolithic MIP-CSP for chiral separation of nateglinide and L-enantiomer. Furthermore, the monolithic nateglinide-MIP exhibited good properties for rapid and efficient enantioseparation over the bulk MIP.

2. Experimental

2.1. Chemicals

Nateglinide, *N*-(*trans*-4-isopropyl-cyclohexylcarbonyl)-L-phenylalanine (L-enantiomer), *N*-(*cis*-4-isopropyl-cyclohexylcarbonyl)-D-phenylalanine (*cis*-isomer) and *trans*-4-isopropylcyclohexanecarboxylic acid (*trans*-acid) were donated by Jiheng Pharmaceutical Co. (Hebei, China). Methanol and acetonitrile (HPLC grade) were purchased from Fisher (New Jersey, USA). Ethylene dimethacrylate (EDMA) from Acros (New Jersey, USA) was extracted with 2 mol l^{-1} NaOH solution and water and dried over anhydrous magnesium sulfate. Acrylamide (AM) and methacrylic acid (MAA) of analytical grade were purchased from

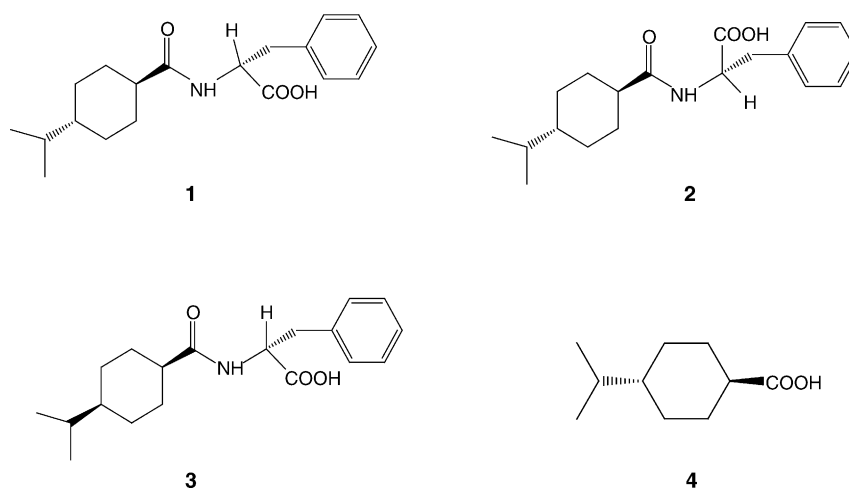


Fig. 1. Structures of nateglinide and related compounds. **1**: *N*-(*trans*-4-isopropyl-cyclohexylcarbonyl)-D-phenylalanine (nateglinide), **2**: *N*-(*trans*-4-isopropyl-cyclohexylcarbonyl)-L-phenylalanine (L-enantiomer), **3**: *N*-(*cis*-4-isopropyl-cyclohexylcarbonyl)-D-phenylalanine (*cis*-isomer), **4**: *trans*-4-isopropylcyclohexanecarboxylic acid (*trans*-acid).

Beijing Chemical Reagent Company (Beijing, China). 2,2'-Azobisisobutyronitrile (AIBN) was purchased from Shanghai Chemical Plant (Shanghai, China). MAA was distilled and AIBN was recrystallized prior to use. Analytical grade cyclohexanol and 1-dodecanol were used without further purification. Unless otherwise specified, all solutions were prepared from a Millipore system (resistivity 18.2 M Ω cm) and filtered through a 0.45 μ m membrane filter from Millipore before use.

2.2. Polymer preparation

The monolithic nateglinide imprinted polymers and non-imprinted polymer (NIP) were synthesized using an in situ polymerization. The template was dissolved in 1.0 ml acetonitrile, the functional monomer acrylamide, cross-linker EDMA and porogenic solvents (cyclohexanol and 1-dodecanol) were added in steps. The mixture was saturated with nitrogen for 10 min and degassed under vacuum for 5 min and then filled into a 150 mm \times 4.6 mm i.d. steel column. The steel column was sealed and put into a 50 $^{\circ}$ C water bath for 24 h. After polymerization, the column was connected to a PU-1580 pump and washed exhaustively on-line with acetic acid/methanol (1:4, v/v), methanol, methanol/triethylamine (999:1, v/v) and finally acetonitrile until no residue of nateglinide was found in the rinses, for complete removal of porogen and the imprinted molecules. The NIP, blank polymer for comparison experiments was prepared similarly to the process described above, except that the polymerization mixture did not contain the imprinted molecule. A bulk MIP was also prepared using in contrast experiments according to our previous study [25] and subsequently fabricated into granules (25–38 μ m). Table 1 summarized the MIPs and NIPs preparation methods.

2.3. Chromatographic evaluation

High performance liquid chromatography was performed on the JASCO chromatographic system consisting of a PU-1580 pump, a variable wavelength UV-1570 detector (JASCO, Japan), equipped with a Rheodyne 7225 injector with a 20 μ l loop. Data processing was carried out with a HW2000 chromatography workstation (Nanjing Qianpu Software Co., China). A CS501-SP thermostat was from Sida

Experimentation Apparatus Factory (Chongqing, China). Acetonitrile was used as the mobile phase and the flow-rate was 1.0 ml min $^{-1}$. The detection was performed at 210 nm, which was the maximum absorption wavelength of nateglinide. Retention factors were calculated from the equation $k' = (t_R - t_0)/t_0$, where t_R is the retention time of retained samples and t_0 is the retention time of the void marker (acetone). The apparent enantioselectivity factor (α) is calculated from the equation $\alpha = k'_D/k'_L$, where k'_D and k'_L are retention factors of nateglinide and its L-enantiomer. The results are listed in Table 1.

2.4. Binding capacity

The binding capacity of the monolithic MIP was investigated by frontal analysis method. The mobile phase was acetonitrile with a flow-rate of 0.5 ml min $^{-1}$. A series of 2 ml volume of different concentrations (0.5, 1.0, 2.0, 3.0, 4.0, 5.0 mM) of nateglinide was prepared and individually injected using a 2 ml loop at ambient temperature. The effective number of binding sites (B_t) and the dissociation constant (K_d) was calculated using the equation [26]:

$$\frac{1}{[A]_0(V - V_0)} = \frac{K_d}{[A_0]B_t} + \frac{1}{B_t} \quad (1)$$

where $[A]_0$ is the concentration of the analyte, V and V_0 are the elution volume of the substrate and the void volume of the monolithic MIP, respectively. The experimental data were processed according to Eq. (1) and $(1)/[A]_0(V - V_0)$ was plotted versus $1/[A]_0$. B_t and K_d could be calculated from the intercepts on the ordinate ($1/B_t$) and the abscissa ($-1/K_d$).

2.5. Morphology analysis

Pore volumes and surface area were determined by nitrogen adsorption on ASAP 2020M system (Micromeritics, USA). The nateglinide-imprinted monolith and NIP were ground and sieved to small particles and selected portion of diameter 25–38 μ m to analysis. The measured data can be processed using software packets, which allow to calculate BET surfaces (seven-point linear plot), micropore (range from 0.5 to 1.7 nm), mesopore (1.7–300 nm) and macropore volumes and pore surfaces or pore size distributions. The average pore diameters were estimated by BJH method.

Table 1
Chromatographic and morphologic performances of imprinted and non-imprinted polymers

P no.	Nateglinide (mmol)	MAA (mmol)	AM (mmol)	EDMA (mmol)	k'_D	α	R_s
P1	1	4	0	20	0.88	1.51	0.6
P2	1	0	4	20	3.39	2.53	1.6
P3	1	6	0	30	0.73	1.28	0.5
P4	1	0	6	30	5.21	2.96	2.4
P5	1	3	3	30	0.64	1.21	–
NIP	0	0	6	30	0.55	1.00	–
P_{bulk}	1	0	6	30	7.52	1.77	0.9

HPLC conditions: column size, 150 mm \times 4.6 mm i.d.; mobile phase, acetonitrile; flow rate, 1.0 ml/min; column temperature, 25 $^{\circ}$ C, detection, 210 nm; loaded amount, 50 nmol.

Scanning electron microscope (SEM) images of the monolithic MIP microstructures were obtained on KYKY-2008B scanning electron microscope.

3. Results and discussion

3.1. Chiral separation on the monolithic MIP-CSP

The monolithic nateglinide-MIPs were prepared by non-covalent imprinting. Nateglinide and its L-enantiomers were chiral separated on this kind of CSP. As shown in Table 1, P2 and P4 (based on acrylamide as functional monomer) have higher apparent enantioselective factors than P1 and P3 (based on MAA). This is due to the strength and stability of the non-covalent interactions, i.e. hydrogen bond, between the template and monomers. Previous studies suggest that an amide group has a stronger hydrogen binding ability than that of methacrylic acid in polar solvents [27,28]. Acetic acid has a dielectric constant value of 6.20, while acetamide has a value of 67.6. The dipole moment of acetic acid is 1.70 D, while for acetamide this value is 3.76 D. The significant differences in the dielectric constants and the dipole moment between acetamide and acetic acid suggest that the amide group ($-\text{CONH}_2$) may form stronger hydrogen bonds with the template than carboxylic group ($-\text{COOH}$) in polar solvents. Therefore, acrylamide has been chosen as the functional monomer in the preparation of nateglinide-MIPs.

Results suggest that a ratio of nateglinide/acrylamide = 1:6 could achieved better enantioseparation. In addition, combined monomers of acrylamide and methacrylic acid were used in the preparation of nateglinide-MIP and the final polymer (P5) showed no better chiral separation than P2 or P4. The apparent enantioselectivity factor illustrated the appropriate strategy – P4 – for nateglinide-MIP preparation.

The enantioselectivity of the monolithic MIP was evaluated by comparing the retention of the enantiomers on this CSP. As shown in the chromatogram (Fig. 2), nateglinide and L-enantiomer were baseline separated on the imprinted polymer CSPs, but no enantioseparation was observed in NIP in the control experiments. When acetonitrile was used as the eluent, the retention factor of nateglinide on the imprinted monolith was 5.21, but only 1.76 for its L-enantiomer.

To evaluate the recognition properties of MIP-CSPs, *cis*-isomer of nateglinide and *trans*-acid were tested on the imprinted monolithic CSPs (Fig. 2). It was found that the *cis*-isomer, containing D-phenylalanine, showed a slightly stronger retention than that of L-enantiomer, while the *trans*-acid showed weak retention on the MIP-CSPs. As far as the analytes are concerned, since their chemical composition and functional groups are the same, they can be distinguished from their steric structures. Nateglinide contains D-phenylalanine unit whereas its L-enantiomer contains L-phenylalanine. In relation to the results of this study, it can be assumed that D-phenylalanine part of

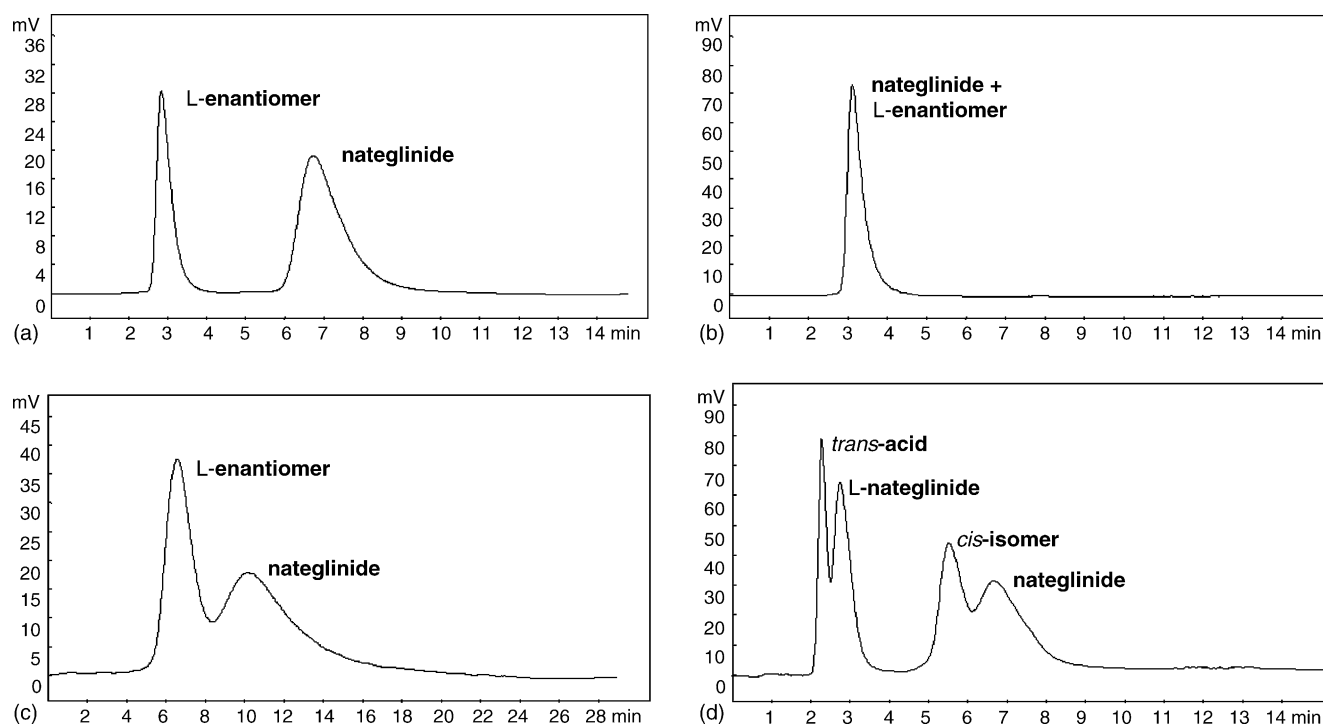


Fig. 2. Separation of nateglinide and related compounds on the polymers. (a) Enantioseparation of nateglinide and L-enantiomer on monolithic MIP. (b) Enantioseparation of nateglinide and L-enantiomer on NIP. (c) Enantioseparation of nateglinide and L-enantiomer on bulk MIP. (d) Separation of the analytes on monolithic MIP. HPLC conditions: column size, 150 mm \times 4.6 mm i.d.; mobile phase, acetonitrile; flow rate, 1.0 ml/min; column temperature, 25 $^{\circ}$ C, detection, 210 nm; loaded amount, 50 nmol.

the template played a crucial role in both the formation of template-monomer complex, and enantiorecognition.

Enantioseparation on bulk MIP was also evaluated by contrast experiments. Fig. 2(c) shows broad and conjoint (resolution=0.9) peaks of the enantiomers. This could be due to the low mass transfer originating from irregularly shaped and sized particles in the packed column. In contrast, the monolithic MIP gave sharper and symmetrical peaks, and resulting in rapid and high efficiency analyses.

3.2. Effects on chiral separation

The influence of mobile phase composition on the chiral recognition properties of nateglinide MIPs was investigated. Using methanol, acetonitrile and 2-propanol, it was shown that only acetonitrile produced satisfactory separation. The effects of polar additives in the mobile phase were also evaluated. A change from 0:100 to 80:20 (v/v) water–acetonitrile proportion suggest that retention factor decreases with the increased proportion of water in the mobile phase. Furthermore, the addition of acetic acid (HOAc) in the mobile phase also resulted in low enantioselectivities and low resolutions. The apparent enantioselectivity factor (α) decreased from 2.96 to 1.72 when 0.25% (v/v) HOAc was in acetonitrile, and further decreased to 1.16 when 0.50% (v/v) HOAc was in the eluent. Therefore, α decreased with the increase of water or acetic acid proportion in the mobile phase, indicating that polar additives can interfere with the hydrogen-bonding interactions between matrix in MIP and the functional group of the analytes.

The continuous and porous structure of monolithic MIP allows for operation at higher flow rates with relatively low backpressures. The influence of flow rate on enantioseparation was measured at a range from 0.2 to 8.0 ml/min. As the flow rate varied from 0.2 to 2.0, α was decreased from 3.56 to 2.72, and when it varied from 2.0 to 8.0 ml/min the decreasing tend of α became flat (from 2.72 to 2.66).

To investigate the effect of temperature on the enantioseparation, the temperature-dependence of the retention factors of the enantiomers was studied. Five replicate injections were made for each analyte at a flow rate of 1.0 ml/min with temperatures 15, 25, 35, 45, 55 °C, respectively. The column was equilibrated with the mobile phase for about 30 min following each temperature change. It was found that both k'_D and k'_L decreased with increasing temperature (Fig. 3). This is because analytes have weaker adsorption to the substrate as temperature increases and therefore migrates faster through the MIP-CSP. Furthermore, the apparent enantioselectivity factors decreased with increasing elution temperature, due to higher temperature decreasing the interaction between the imprinted molecule and the polymers more than the interaction between non-imprinted molecule and the polymers. Therefore, a lower temperature will lead a higher enantioselectivity.

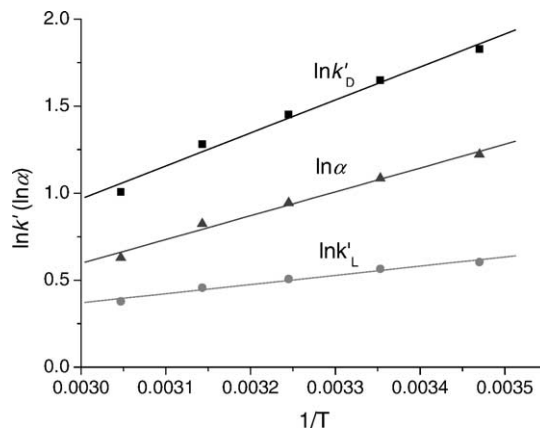


Fig. 3. Van't Hoff plots by plotting $\ln k'$ vs. $1/T$.

3.3. Binding capacity

To better understand the binding capacity of nateglinide-MIPs, the effective number of binding sites (B_t) and the dissociation constant (K_d) were determined using the frontal analysis method. According to Eq. (1), when the concentration of nateglinide is known, V_0 and V can be calculated from the product of void time and retention time multiplied by the flow rate. The retention times of the break-through curves were obtained from the times at half-height of the plateaus. The experimental data were treated according to Eq. (1), and the results were shown in Fig. 4. The monolithic nateglinide-MIP has number of binding sites $B_t = 41.15 \mu\text{mol g}^{-1}$ with a dissociation constant of $K_d = 7.40 \text{ mM}$.

3.4. Thermodynamics of chiral separation

Kim and Guiochon [21,29,30] investigated the thermodynamic properties of particulate and monolithic MIPs using adsorption isotherm models and expectation maximization (EM) method. In this paper, we discuss the thermodynamic properties of chiral separation on monolithic MIP in relation to temperature.

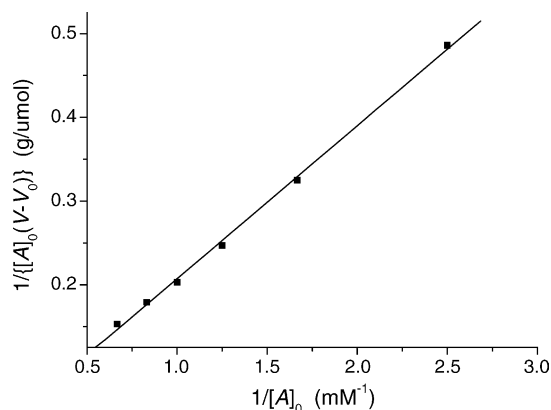


Fig. 4. Plot of $1/[A]_0(V - V_0)$ vs. $1/[A]_0$ for the monolithic nateglinide-MIP.

Table 2
Thermodynamic parameters of the chiral separation on nateglinide-MIP monolith

Analytes	ΔH (kJ mol ⁻¹)	$\Delta S'$ (J mol ⁻¹ K ⁻¹)	$\Delta\Delta H$ (kJ mol ⁻¹)	$\Delta\Delta S$ (J mol ⁻¹ K ⁻¹)
Nateglinide	-15.76	-39.22	-11.37	-29.17
L-Enantiomer	-4.38	-10.08		

ΔH and $\Delta S'$ ($\Delta S' = \Delta S + R \ln \phi$) were obtained from linear regression of the Van't Hoff plots by plotting $\ln k'$ vs. $1/T$; $\Delta\Delta H$ and $\Delta\Delta S$ were obtained from plot of $\ln \alpha$ vs. $1/T$.

The retention behavior and thermodynamic parameters determined in this study were used to estimate the enthalpy, entropy, and Gibbs free energy of association between the enantiomers and the CSP. Data obtained from chiral separation at temperatures ranging from 15 to 55 °C were processed using the Van't Hoff equation [5,29] to estimate the thermodynamic properties of the separation.

$$\ln k' = -\frac{\Delta H}{RT} + \frac{\Delta S}{R} + \ln \phi \quad (2)$$

$$\ln \alpha = -\frac{\Delta\Delta H}{RT} + \frac{\Delta\Delta S}{R} \quad (3)$$

where R , T and ϕ are the gas constant, the absolute temperature and the phase volume ratio, respectively. Enthalpy (ΔH) and entropy (ΔS), enthalpy difference ($\Delta\Delta H$) and entropy difference ($\Delta\Delta S$) can be calculated from the slopes and intercepts of linear portion of corresponding Eqs. (2) and (3). The results are listed in Table 2.

The absolute values of ΔH and $\Delta S'$ (i.e. $|\Delta H|$ and $|\Delta S'|$) for nateglinide were larger than those of L-enantiomer. This suggests that nateglinide has stronger affinity to the recognition sites, and could form a more stable template-MIP complex than L-enantiomer during their matching in the micro-cavities on the MIP. Moreover, the fact that $|\Delta\Delta H| > T|\Delta\Delta S|$ indicates that the chiral separation on this monolithic MIP-CSP was an enthalpy-controlled process. The Van't Hoff plots of the two enantiomers (Fig. 3), shows a large difference in slopes that corresponded to $\Delta\Delta H$. That is, the two lines are diverging from each other. In general, for the temperature range of 15–55 °C, the enthalpic contribution to the overall substrates transfer energy was found to be more significant than the entropic one. In this case, the decrease in temperature led to an increase of enantioseparation factors. This result is consistent with the results of the temperature-dependence experiment.

3.5. Morphological characteristics of nateglinide imprinted monolith

Morphological analysis including pore analysis and SEM analysis of the polymers were also investigated in this experiment.

3.5.1. Pore analysis

Nitrogen adsorption experiments were performed and the specific surface areas (A), specific pore volumes (V) and average pore diameter (d_p) of nateglinide-MIPs were obtained.

The NIP was analyzed as control experiment to demonstrate the differences between imprinted and non-imprinted monoliths. Results indicate the specific surface areas; specific pore volumes and average pore diameter were 286.5 m²/g, 0.654 cm³/g and 9.1 nm for monolithic MIP, and 239 m²/g, 0.512 cm³/g and 8.6 nm for NIP, respectively. Obviously, the BET surface area of the imprinted monolith is higher than that of NIP.

3.5.2. SEM analysis

It can be seen from the SEM image (Fig. 5) that there are many macropores and flow-through channels inlaid in the network skeleton of nateglinide-imprinted monolith. These macropores and channels allowed mobile phase to flow through the monolith with low flow resistance, and thus enables fast mass transfer of the solutes. The low backpressure allows their operation at higher flow rates. The relationship of backpressure versus flow rate on the monolithic MIP showed that even at the high flow rate of 5.0 ml/min, the backpressure was only 7.36 MPa (Fig. 6). In contrast, the backpressure of P_{bulk} was relatively much higher over the whole range of flow rate, due to the irregular shape and non-uniform sizes of packed particles.

The good morphologic properties for the monolithic MIP were more likely originated from the polymerization process. There are at least three factors that should be taken into account: the polymerization temperature, the composition of

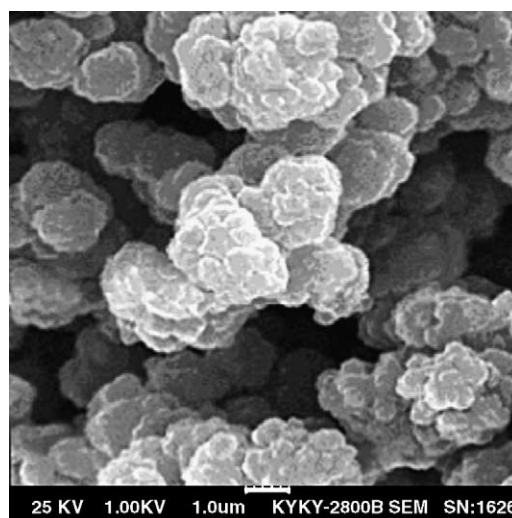


Fig. 5. Scanning electron microscope (SEM) of monolithic MIP (P4).

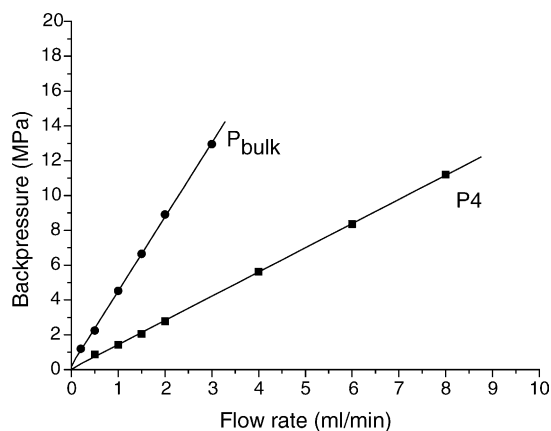


Fig. 6. Relationship of backpressure vs. flow rate on the monolithic MIP (P4) and bulk MIP (P_{bulk}).

pre-polymerized solution (e.g. the type and amount of cross-linker) and the porogenic solvent, which were related to the phase separation process. The influence of temperature on pore size and the influence of various compositions of pre-polymerized solution on the porosity and specific surface area were detailed in previous work [31–33]. Temperature is regarded as the most convenient variable to adjust the pore size distribution of macroporous media because it does not result in changes in the composition of the reaction mixture. It was believed that temperature could affect the polymer morphology in different ways, e.g. generating free radicals and forming cross-linked nuclei, due to complexity of the phase separation. The influences of various degrees of crosslinking and of monomer concentration on the porosity, specific surface area and the structure of the final polymers were discussed in detail by Glad et al. [10].

Besides the temperature and proportion of the prepolymeric mixture, the porogenic solvents also play an important role in the morphology of the molecularly imprinted monolith in terms of specific surface area and pore size. The porogenic solvents must have good solvency for the imprinted molecules, and will not destroy the interaction between the imprinted molecules and functional monomers. On the other hand, during the phase separation process of polymerization, the porogenic solvents should redound to form the crosslinking network with high macroporosity. According to these results, the preparation of monolithic MIP was performed under relatively strict conditions as described in Section 2.2. The typical nateglinide MIP-P4 was prepared in a steel column as: 1.0 mmol nateglinide; 6.0 mmol AM; 30 mmol EDMA; porogenic solvents: acetonitrile 2.4 ml, cyclohexanol 3.6 ml, 1-dodecanol 6.0 ml; polymerization temperature, 50 °C. However, according to the traditional crafts, the bulk MIP was synthesized in a conical flask only using 10.0–12.0 ml acetonitrile, and the recognition sites were partially buried in the body of bulk, leading an inhomogeneous distribution of recognition sites.

4. Conclusions

Monolithic nateglinide-MIPs used as chiral stationary phase were prepared using an in situ method. Nateglinide and its enantiomer were successfully separated on this kind of monolithic MIP-CSP. Experiments showed that chiral recognition was dependent on the stereo structures and the arrangement of functional groups on the cavities of the MIP. The thermodynamics of the enantioseparation indicated that the enantioseparation was an enthalpy-controlled process. In contrast to bulk nateglinide-MIP, monolithic nateglinide-MIPs showed unique properties: ease of preparation; all binding sites beyond destruction during grinding; fast mass transport and hence rapid separation; homogeneous and continuous construction and hence lower pressure drops, high efficiencies even at high flow rate.

The monolithic MIP possesses homogeneous structure with both mesopores and through pores. From a morphologic point of view, this can provide better enantioseparation by reducing the nonselective binding sites. Further more, the high penetrability and low backpressure allow a rapid enantiomeric recognition.

Acknowledgements

This work was supported by National Natural Science Foundation of China (grant no.20375010, no. 20435030), “Bairen” Project of Chinese Academy of Sciences, Excellent Youth Program of Chinese Education Ministry.

References

- [1] G. Wulff, *Angew. Chem. Int. Ed. Engl.* 34 (1995) 1812.
- [2] M. Kempe, K. Mosbach, *J. Chromatogr. A* 694 (1995) 3.
- [3] A.M. Esteban, *Fresenius J. Anal. Chem.* 370 (2001) 795.
- [4] R. Suedee, T. Srichana, G.P. Martin, *J. Control. Relea.* 66 (2000) 135.
- [5] B. Sellergren, K.J. Shea, *J. Chromatogr. A* 690 (1995) 29.
- [6] C. Yu, K. Mosbach, *J. Chromatogr. A* 888 (2000) 63.
- [7] Y. Lu, C. Li, H. Zhang, X. Liu, *Anal. Chim. Acta* 489 (2003) 33.
- [8] J. Haginaka, C. Kagawa, *J. Chromatogr. B* 804 (2004) 19.
- [9] L. Zhang, G. Cheng, C. Fu, *React. Funct. Polym.* 56 (2003) 167.
- [10] M. Glad, P. Reinholdsson, K. Mosbach, *React. Polym.* 25 (1995) 47.
- [11] C. Sulitzky, B. Ruckert, A.J. Hall, F. Lanza, K. Unger, B. Sellergren, *Macromolecules* 35 (2002) 79.
- [12] F. Svec, J.M. Frechet, *Anal. Chem.* 64 (1992) 820.
- [13] H. Minakuchi, K. Nakanishi, N. Soga, N. Ishizuka, N. Tanaka, H. Koyabashi, *Anal. Chem.* 68 (1996) 1275.
- [14] A.M. Siouffi, *J. Chromatogr. A* 1000 (2003) 801.
- [15] J. Matsui, T. Kato, T. Takeuchi, M. Suzuki, K. Yokoyama, E. Tamiya, I. Karube, *Anal. Chem.* 65 (1993) 2223.
- [16] J. Matsui, I.A. Nicholls, T. Takeuchi, *Anal. Chim. Acta* 365 (1998) 89.
- [17] L. Schweitz, L.I. Andersson, S. Nilsson, *Anal. Chem.* 69 (1997) 1179.
- [18] J. Nilsson, P. Spegel, S. Nilsson, *J. Chromatogr. B* 804 (2004) 3.
- [19] X. Huang, H. Zou, X. Chen, Q. Luo, L. Kong, *J. Chromatogr. A* 984 (2003) 273.

- [20] X. Huang, F. Qin, X. Chen, Y. Liu, H. Zou, J. Chromatogr. B 804 (2004) 13.
- [21] H. Kim, G. Guiochon, Anal. Chem. 77 (2005) 93.
- [22] E.S. Horton, C. Clinkingbeard, M. Gatlin, J. Foley, S. Mallows, S. Shen, Diabetes Care 23 (2000) 1660.
- [23] M. Qi, P. Wang, Y. Sun, Y. Li, J. Liq. Chromatogr. Related Technol. 26 (2003) 1839.
- [24] G. Yang, Z. Li, D. Wang, Z. Zhang, E. Liu, Y. Chen, Chromatographia 56 (2002) 515.
- [25] G. Yang, J. Yin, Z. Li, H. Liu, L. Cai, D. Wang, Y. Chen, Chromatographia 59 (2004) 705.
- [26] H. Li, L. Nie, S. Yao, Chromatographia 60 (2004) 425.
- [27] C. Yu, K. Mosbach, J. Org. Chem. 62 (1997) 4057.
- [28] T. Zhang, F. Liu, W. Chen, J. Wang, K. Li, Anal. Chim. Acta 450 (2003) 53.
- [29] H. Kim, G. Guiochon, Anal. Chem. 77 (2005) 1708.
- [30] H. Kim, G. Guiochon, Anal. Chem. 77 (2005) 1718.
- [31] J. Lin, T. Nakagama, K. Uchiyama, T. Hobo, Biomed. Chromatogr. 11 (1997) 298.
- [32] F. Svec, J.M. Frechet, Macromolecules 28 (1995) 7580.
- [33] Y. Lu, C. Li, X. Wang, P. Sun, X. Xing, J. Chromatogr. B 804 (2004) 53.